Available online at www.sciencedirect.com

ScienceDirect

Advances in Space Research xxx (2019) xxx–xxx

ADVANCES IN SPACE RESEARCH (a COSPAR publication)

www.elsevier.com/locate/asr

Characterisation of Total Electron Content over African region using Radio Occultation observations of COSMIC satellites

Patrick Mungufeni [a,*], Babatunde A. Rabiu [b], Daniel Okoh [b], Edward Jurua [a]

[a] Physics Department, Mbarara University of Science and Technology, P.O. Box 1410, Mbarara, Uganda
[b] Centre for Atmospheric Research, National Space Research and Development Agency, Anyigba, Nigeria

Received 6 December 2018; received in revised form 27 June 2019; accepted 8 August 2019

Abstract

This study characterised the Total Electron Content (TEC) over the African region during the years 2008–2015. The TEC data used were the integrated electron density observed during Radio Occultation (RO) event associated with Constellation Observing System for Meteorology, Ionosphere and Climate (COSMIC) satellites. These TEC data were referred to as COSMIC TEC. The results indicate that the COSMIC TEC captures the well known features of the ionosphere such as: (i) occurrence of minimum and maximum TEC during 0:00–08:00 LT and 12:00–16:00 LT respectively, (ii) occurrence of secondary TEC enhancement (maximum) during 16:00–20:00 LT, (iii) lowest TEC values being observed in June solstice and highest TEC values observed in March equinox, (iv) TEC values increase as solar activity changes from low to high, (v) mid latitude TEC values are lower than those of low latitude regions, and (vi) occurrence of equatorial ionisation anomaly. In addition, we validated RO TEC observations of COSMIC satellites using Ground-based Global Navigation Satellite System (GNSS) receiver TEC observations (Ground TEC). To achieve this, we quantified the difference between Ground TEC and COSMIC TEC that were simultaneously observed within the vicinity of the ground receiver. The Upper Quartiles, UQ, of the magnitudes of the differences of coincident COSMIC and Ground TEC over southern mid-latitude regions were <4 TECU, while over low-latitude and northern mid-latitude regions, the values ranged from 6.17 to 11.20 TECU. The high TEC differences over low latitude regions compared to those over southern mid latitudes could have resulted from errors due to the spherical symmetry assumption during the RO retrievals. The question that remains is, why there are large TEC differences over the northern mid-latitude regions. Since COSMIC TEC captures the well known features of the ionosphere, it might in future be used for empirical modeling over African region, thus, making this study crucial.
© 2019 COSPAR. Published by Elsevier Ltd. All rights reserved.

Keywords: Ionosphere; Total Electron Content; COSMIC TEC

1. Introduction

Nowadays, the Global Positioning System (GPS) Radio Occultation (RO) technique is being used to sound the global atmosphere in all weather over both lands and oceans. Examples of Low Earth Orbit (LEO) satellite missions that implemented RO include; the MicroLab 1, the Satellite de Aplicaciones Cientificas-C (SAC-C), the Challenging Minisatellite Payload (CHAMP), the twin Gravity Recovery and Climate Experiment (GRACE), and the FORMOSA Satellite Series Number 3 (FORMOSAT-3)/Constellation Observing System for Meteorology, Ionosphere and Climate (COSMIC). In the ionosphere, the GPS RO technique is primarily used to obtain electron density profiles based on various inversion methods as described in Garcia-Fernadez et al. (2002), Kuo et al. (2003), Jakowski et al. (2004), Pedatella et al. (2015). From electron density profiles, it is possible to determine the F2-layer peak height (hmF2) and electron density (NmF2). Examples of ionospheric studies that have used GPS RO data are those of Hoque and Jakowski (2012),

* Corresponding author.
E-mail address: pmungufeni@gmail.com (P. Mungufeni).

https://doi.org/10.1016/j.asr.2019.08.009
0273-1177/© 2019 COSPAR. Published by Elsevier Ltd. All rights reserved.

Please cite this article as: P. Mungufeni, B. A. Rabiu, D. Okoh et al., Characterisation of Total Electron Content over African region using Radio Occultation observations of COSMIC satellites, Advances in Space Research, https://doi.org/10.1016/j.asr.2019.08.009

Krankowski et al. (2011), Yue et al. (2015). The results show that comparison of electron density profiles determined by RO technique are usually in good agreement with those determined by ground based ionosondes.

Apart from using RO technique for studying the ionosphere, some studies have used ground-based Global Navigation Satellite System (GNSS) receivers and ionosondes to measure the Total Electron Content (TEC). Over the African region, such data has been used to characterise TEC over specific locations or regions (Adewale et al., 2012; Obrou et al., 2009; Akala et al., 2013; Olwendo et al., 2016). The results indicate that over the equatorial region of the African continent, the VTEC generally increases from 06:00 LT and reaches its maximum value approximately during 15:00–17:00 LT (Adewale et al., 2012). Over Korhogo (geog lat = 9.33°N, geog lon = 5.43°W, dip lat = 0.67°S), the TEC has an increasing variation that is linear in the time range from 0600 to 1100 LT, a gradual decrease after 1100 LT until 1800 LT, and after sunset the TEC decreases until mid-night (Obrou et al., 2009). Seasonally, during solar minimum, maximum VTEC values were observed over Lagos, Nigeria (geog lat 6.52° N, geog lon 3.4° E, mag lat 3.04° S) during March equinox and minimum during solstices (Akala et al., 2013). However, during the ascending phase of the solar activity, the maximum values were recorded during the December solstice and minimum during the June solstice. VTEC also increased with solar activity (Akala et al., 2013). The equatorial anomaly crests manifest remarkable seasonal variations over the East African sector. The crest of the EIA was fully formed and yields the maximum values of TEC during the equinoxes (March/April and September/October) and minimum in the solstice (June/July and November/December) (Olwendo et al., 2016).

The studies that are mentioned in the previous paragraph have characterised TEC over specific regions of Africa. This results in knowledge gaps in ionospheric characteristics over some parts of the region. This makes it difficult to develop empirical ionospheric model over the entire African region. Therefore, in this study, we characterised TEC over African region using the integrated TEC from ground up to the orbit of COSMIC satellites. The integrated TEC (COSMIC TEC) were determined using electron density profiles observed by COSMIC satellites. Moreover, we validated COSMIC TEC with the TEC derived using ground based GNSS receivers (Ground TEC). The validation of COSMIC TEC and the characterisation of TEC over African region using it would justify the future use of COSMIC TEC for empirical modeling of TEC over African region. The data sources used in the study are described in the next section.

2. Data sources and the methods

The COSMIC mission launched on April 15, 2006 consists of six LEO micro-satellites assigned mainly for the GPS RO remote sensing of the atmosphere and ionosphere. The six LEO satellites are in different orbital planes. Initially, the orbital altitudes were about 500 km and then raised to the final planned altitude of about 800 km towards the end of the year 2007. More information about the constellation deployment can be found in Chen-Joe (2008) and Syndergaard et al. (2006). In this study, we used the integrated TEC available in ionPrf files which are processed at the COSMIC Data Analysis and Archive Center (CDAAC) (http://cosmic-io.cosmic.ucar.edu/cdaac/index.html). The integrated TEC for the individual occultation events were assigned to the geographic coordinates of NmF2 that are reported in the same file.

As already stated in Section 1, we validated COSMIC TEC using Ground TEC. This was done by comparing the two data sets. The data used for comparison were archived during high solar activity (HSA) years 2012 and 2015. In each of the years, the median F10.7 flux was ~117 sfu. We think that the data within the two years is adequate for statistical analysis to support any conclusion that might be drawn about the validation. The Receiver Independent Exchange (RINEX) data files that were obtained from the International GNSS Service (IGS) stations (http://www.sopac.ucsd.edu) listed in Table 1 were used to derive the Ground TEC. These stations had adequate data during the years 2012 and 2015. The IGS stations listed in Table 1 are distributed within and around the African continent as shown in Fig. 1. Countries where the receivers are located are indicated in column 1 of Table 1. The dotted and dashed lines in Fig. 1 indicate the magnetic equator and the nominal locations (±15° magnetic latitude) of crests of equatorial ionisation anomaly respectively. These lines helped us in comparing the well known patterns of spatial distribution of electron densities around the EIA region with the distribution exhibited in this study. The IGS stations used in the study were chosen such that: ADIS falls within the neighbourhood of the magnetic equator; NKLG, MOIU, LPAL, and SEY1 are within the neighborhood of the EIA crest region; while RABT, LAMPT, BSHM, ZAMB, and SUTH are in the mid-latitudes (outside the EIA region).

The RINEX files obtained from the IGS stations were processed using GPS-TEC analysis software (Seemala and Valladares, 2011) to obtain STEC as a function of Universal Time (UT) and elevation angles of satellites tracked. After removing satellite and receiver biases from STEC, the software maps it to VTEC at the Ionospheric Pierce Points (IPP). The satellite biases are published by the University of Berne in Switzerland (ftp://ftp.unibe.ch/aiub/CODE/). The GPS-TEC analysis software estimates receiver bias for a specific receiver by trying several values and taking the one that gives the minimum summed standard deviation of observed VTEC during 03:00–06:00 LT.

The TEC response to geomagnetic storms can be both positive and negative (Risbeth and Garriot, 1969; Buonsanto, 1999; Adewale et al., 2011). During characterisation of TEC in disturbed geomagnetic conditions, grouping of data according to the types of ionospheric

Please cite this article as: P. Mungufeni, B. A. Rabiu, D. Okoh et al., Characterisation of Total Electron Content over African region using Radio Occultation observations of COSMIC satellites, Advances in Space Research, https://doi.org/10.1016/j.asr.2019.08.009

Table 1
Ground based GNSS receiver Sites used in the study.

Station Name, Country	Station Code	Geog. Coord		Mag. lat (°)
		Lon (°)	Lat (°)	
Rabat, Morocco	RABT	353.1	34.0	23.9
RoquedelosMucha, Spain	LPAL	342.1	28.8	17.6
Haifa, Israel	BSHM	35.0	32.8	26.0
Addis Ababa, Ethiopia	ADIS	38.7	9.0	1.3
Libreville, Gabon	NKLG	9.7	0.35	−8.05
Eldoret, Kenya	MOIU	35.3	0.3	−9.2
Lusaka, Zambia	ZAMB	28.3	−15.3	−26.2
La Misere, Seychelles	SEY1	55.5	−4.7	−13.6
Sutherland, South Africa	SUTH	20.8	−32.3	−41.1
Lampedusa, Italy	LAMP	12.6	35.5	26.6

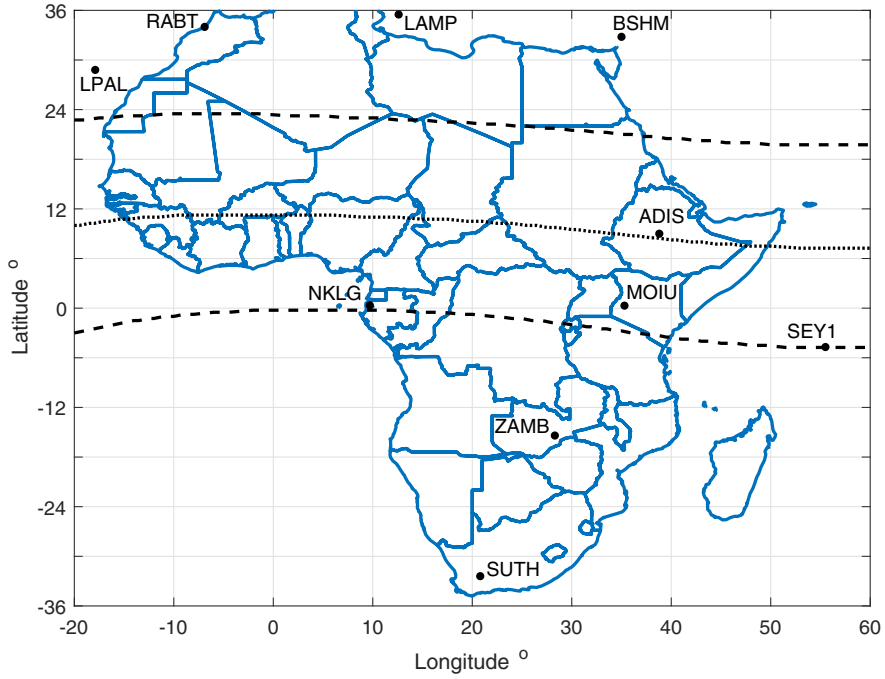


Fig. 1. Map showing distribution of IGS stations used in the study. The dotted and dashed lines represent 0 and ±15° magnetic latitudes, respectively.

response would be necessary. Since all the geomagnetic storms that occurred during the study period are not yet characterised in terms of the possible ionospheric responses, the RINEX and ionPrf files processed in this study were those archived during geomagnetically quiet days. The quiet days were identified when all the Kp values were $\leqslant 3$ on that day. The characterisation of TEC over the African region during disturbed geomagnetic conditions would be done in a separate study.

3. Characterisation of TEC over African Region

The COSMIC TEC data during the years 2008–2015 when COSMIC satellites were in their final planned orbital altitude were used for characterising TEC over the African region. This period also represents data of both low and high solar activity, mostly during sunspot cycle 24. It should be noted that sunspot cycle 23 ended around the year 2009. The data within geographic latitude and longitude ranges of −36 to 36° and −20 to 60° respectively were used in order to cover the African region. The data were binned in grids with resolution of 10° in longitude and 2° latitude. Considering that local time (LT) usually changes after about 15°, the longitude binning resolution was chosen to be within the same LT. On the other hand, the latitude binning resolution was reduced to 2° to cater for the rapid latitudinal TEC changes over the EIA. The COSMIC TEC data might be recorded over some grids a few times (~ 3) in a day. Because of this, in order to acquire enough data for characterisation, the TEC data for the different days were binned according to LT, season, and solar activity level.

For each spatial grid, the data were binned at 1 h interval. TEC values within the bins were averaged to yield 1 h resolution TEC data over the grids. The TEC data for the different days were then binned according to F10.7 flux of that day. As in Mungufeni et al. (2015), the F10.7 flux ranges for low solar activity (LSA), medium solar activity

Please cite this article as: P. Mungufeni, B. A. Rabiu, D. Okoh et al., Characterisation of Total Electron Content over African region using Radio Occultation observations of COSMIC satellites, Advances in Space Research, https://doi.org/10.1016/j.asr.2019.08.009

(MSA), and high solar activity (HSA) bins were < 80, 80–120, and >120 sfu respectively. The data within a specific solar flux bin were further binned based on months of a year.

It is important to emphasize that in this study, we characterised TEC in terms of local time, seasonal, spatial, and solar activity dependence.

3.1. Local time and spatial variation of TEC

In order to show the variation of TEC with LT as well as spatially, we present Fig. 2. In the figure, letters on top indicate the column numbers while roman numbers on the left indicate the row numbers. Panels in columns (a)–(d) correspond to geographic longitudes −15, 5, 25, and 35°, respectively, while panels in rows (i)–(vi) correspond to geographic latitude sectors >27, 15–27, 3–15, −9 to 3, −24 to −9, <−24°, respectively. The latitude sectors were selected to represent locations (i) in mid-latitude (latitude ranges: >27, −24 to −9, and <−24°) (ii) at the crests of EIA (latitude ranges: 15–27, −9 to 3°), and (iii) at the trough of EIA (latitude range: 3–15°). The dots in Fig. 2 show TEC variations on the different days in March during HSA. The median TEC variation in the month is shown by the red line.

It can be seen in most of the panels in Fig. 2 that the minimum TEC values occur during 0:0–08:00 LT. The maximum TEC values mostly appear during 12:00–16:00 LT and 16:00–20:00 LT over latitudes ≤ 27° and > 27°, respectively. These results are similar to those reported over the equatorial region of African by Adewale et al. (2012) (see Section 1). Hargreaves (1992) stated that, whereas the daily peak in TEC may likely occur near noon in the winter, it may occur either before or after local noon in the summer. He further mentioned that the diurnal variation of TEC may be asymmetrical about noon since there can be rapid changes at sunrise but perhaps little or none at sunset. This fact is evidenced in panels in rows (i)–(iv) of Fig. 2. In particular, the TEC values remain fairly high after occurrence of a maximum. The physical processes that create electron density change with LT, resulting into the diurnal variation of the TEC. At sunrise, the electron density begins to increase rapidly owing to photo-ionization (Schunk and Nagy, 2009). After this initial increase at sunrise, electron density displays a slow rise throughout the day, and then it decays at sunset as the photo-ionization source disappears.

Another feature that can be seen in Fig. 2 is the occurrence of a secondary maximum/enhancement of TEC during 16:00–20:00 LT. Typical examples are panels in rows

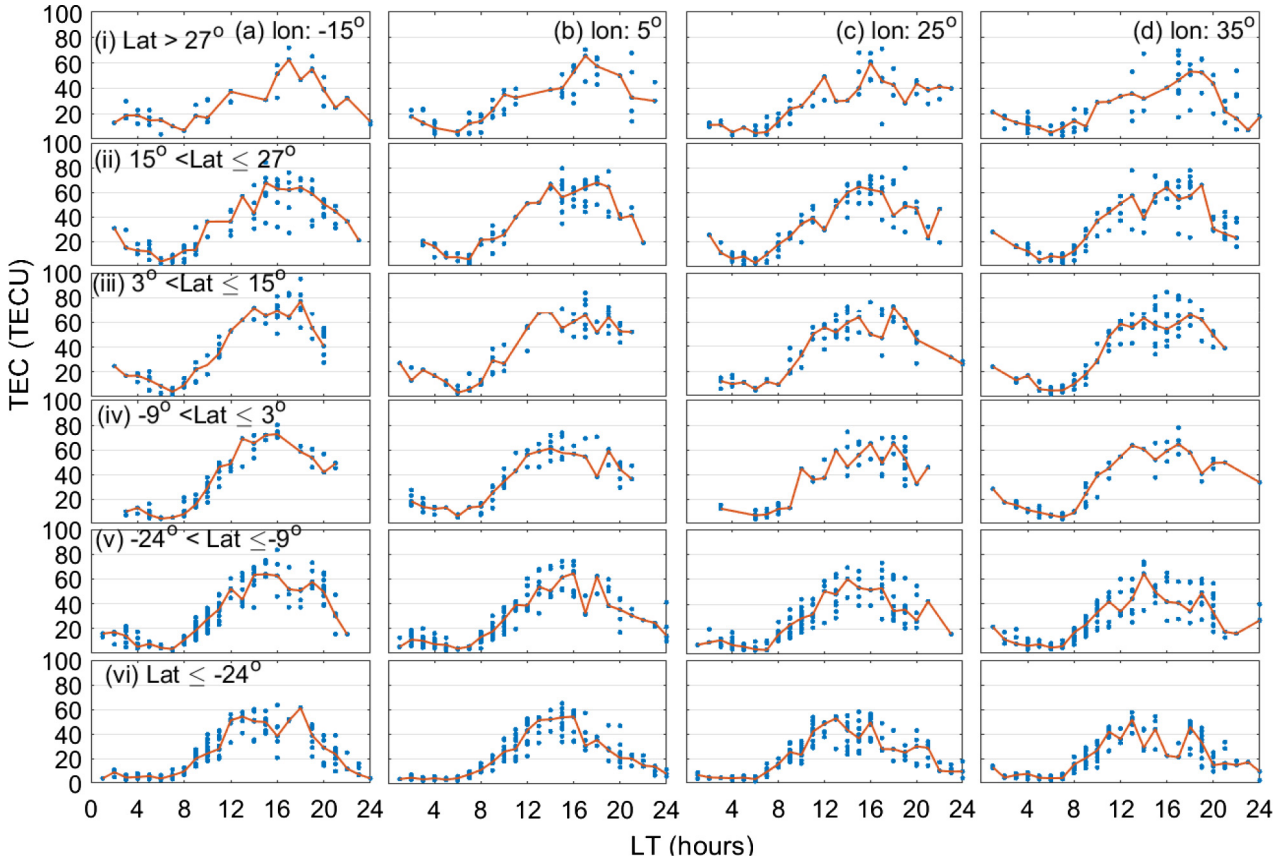


Fig. 2. Diurnal Variation of TEC over longitudes, −15, 5, 25, and 35°. Panels in columns (a)–(d) correspond to the selected longitudes, maintaining the order of their enumeration. Panels in rows (i)–(vi) correspond to latitude sectors >27, 15–27, 3–15, −9–3, −24 to −9, <−24°, respectively.

Please cite this article as: P. Mungufeni, B. A. Rabiu, D. Okoh et al., Characterisation of Total Electron Content over African region using Radio Occultation observations of COSMIC satellites, Advances in Space Research, https://doi.org/10.1016/j.asr.2019.08.009

(v)–(vi) of column (a), rows (iv)–(v) of column (b), and row (iii) of column (c). The probable scenario leading to the formation of a secondary maximum during the stated LT is as follows. During the day, the thermospheric wind generates a dynamo electric field in the lower ionosphere that is eastward (Schunk and Nagy, 2009). The eastward electric field, E in combination with the northward geomagnetic field, B produces an upward E × B drift of the F region plasma. As the ionosphere co-rotates with the Earth toward dusk, the zonal (eastward) component of the neutral wind increases. The increased eastward wind component, in combination with the sharp day-night conductivity gradient across the terminator leads to the pre-reversal enhancement in the eastward electric field (Batista et al., 1986; Schunk and Nagy, 2009). The F layer therefore rises as the ionosphere co-rotates into darkness. Although in the absence of sunlight after sunset, the lower ionosphere rapidly decays, there exists high electron density at high altitudes, yielding the secondary maximum in TEC.

The locations outside the EIA region (panels in rows (i) and (vi) of Fig. 2) indicate occurrence of TEC values mostly ⩽60 TECU. On the other hand, locations around and within the EIA region (see panels in rows (ii)–(iv) of Fig. 2) present several cases of TEC values ⩾60 TECU. The low values of TEC over locations outside the EIA region might be due to low solar radiation flux which is responsible for creation of electrons (Schunk and Nagy, 2009). The solar radiation flux is usually low for locations far from the sub-solar point. The latter situation is dominant over locations outside the EIA region, especially in March. The closeness of the sub-solar point to the locations within the EIA regions result into high solar radiations over these locations. As a result, high TEC values were observed over locations within the EIA region.

3.2. Dependence of TEC on solar flux

The variation of TEC with solar activity is illustrated in Fig. 3. In the figure, panels (a)–(c) show the variation of TEC as a function of longitude and latitude during HSA, MSA, and LSA respectively. The TEC values presented are the average values during 13:00–14:00 LT for days in March. The magenta line represents the magnetic equator. The white spaces within the panels in Figs. 3 and 4 show missing data. Table 2 shows the number of days with data in the various months presented in Figs. 3 and 4. The average TEC data in a month that has more days can be trusted more. It can be seen in Table 2 that the three months presented in Fig. 3 all have adequate data (>60 days).

It can easily be seen in Fig. 3(c), the lowest TEC values occur during LSA, while the highest occur during HSA period (see Fig. 3(a)). This observation is due to the fact

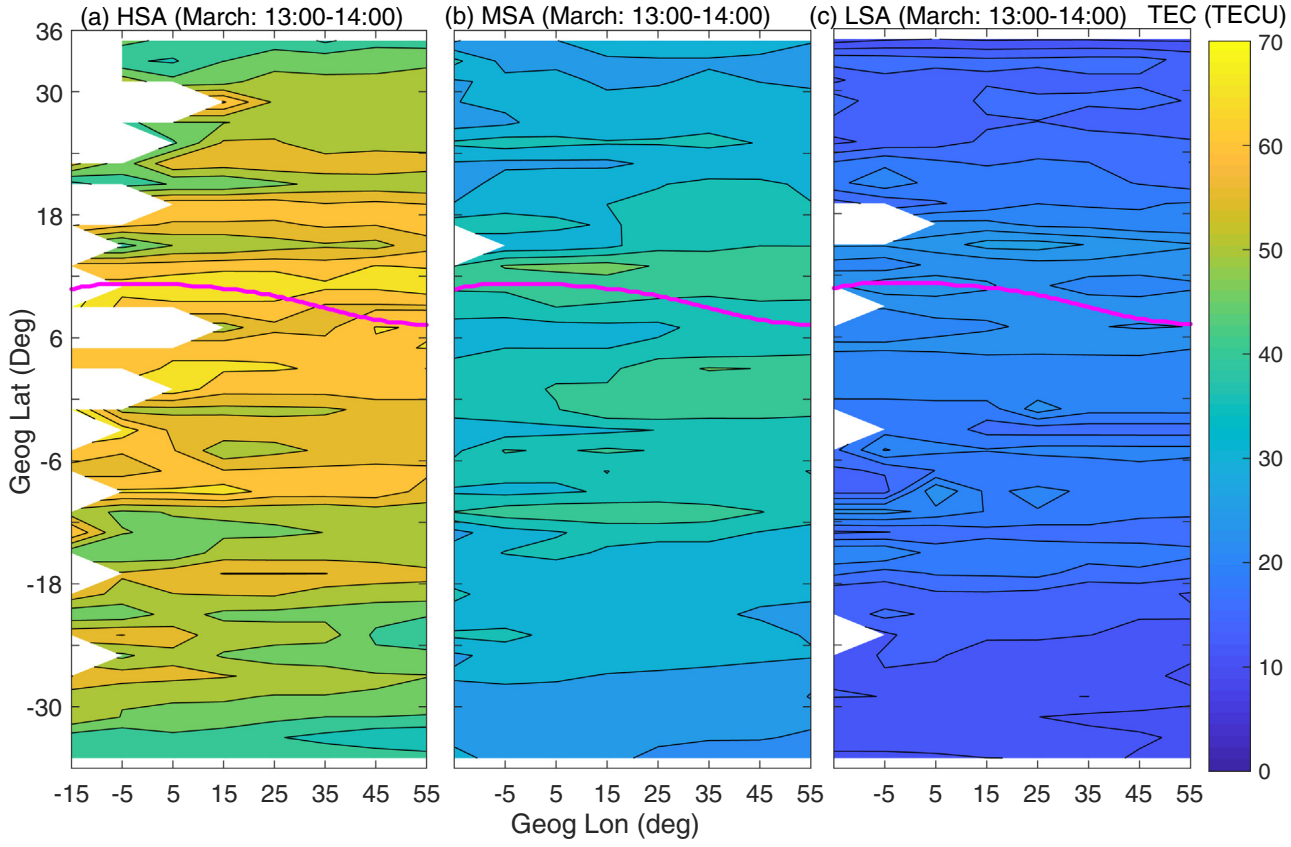


Fig. 3. Variation of TEC as a function of geographic longitude and latitude in March during 13:00–14:00 LT. Panels (a)–(c) are for HSA, MSA, and LSA periods respectively. The magenta line shows the magnetic equator. (For interpretation of the references to colour in this figure legend, the reader is referred to the web version of this article.)

Please cite this article as: P. Mungufeni, B. A. Rabiu, D. Okoh et al., Characterisation of Total Electron Content over African region using Radio Occultation observations of COSMIC satellites, Advances in Space Research, https://doi.org/10.1016/j.asr.2019.08.009

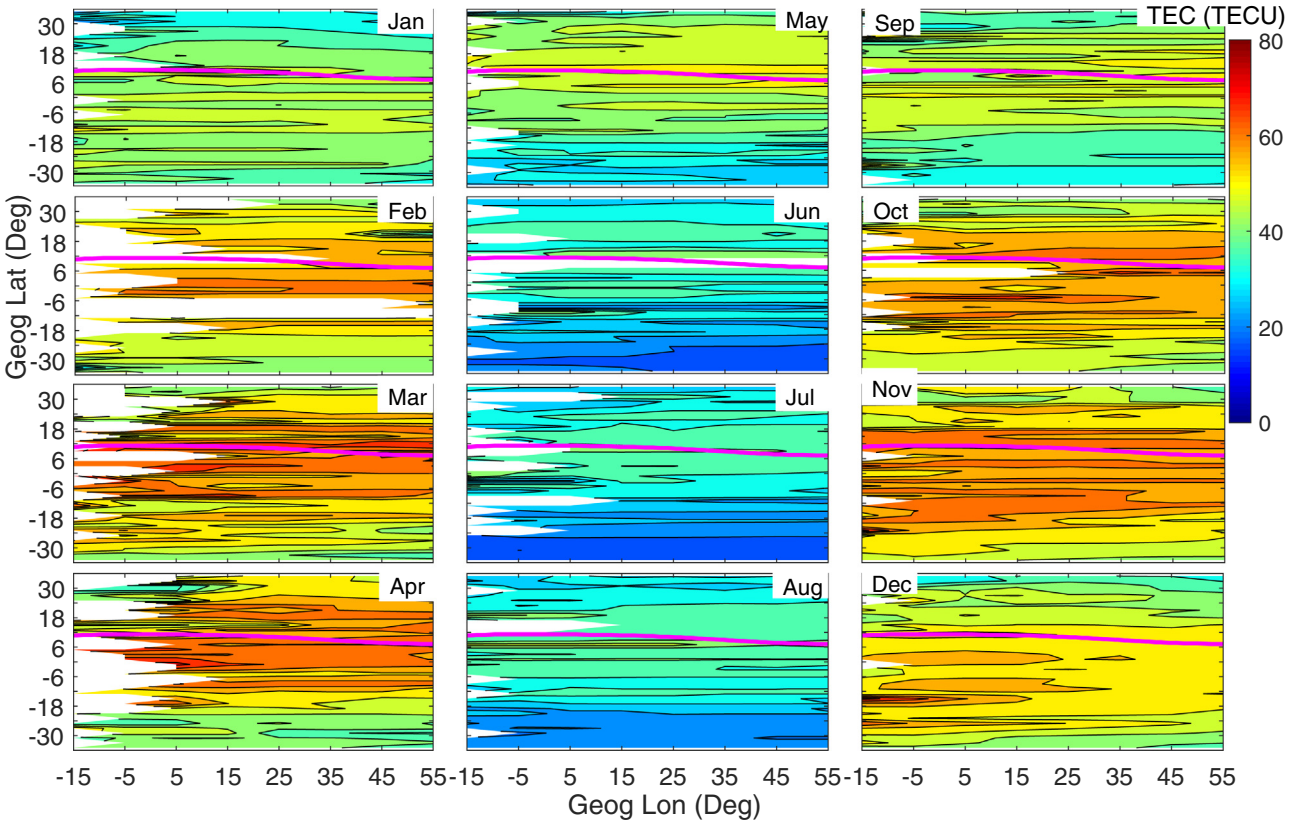


Fig. 4. Variation of TEC as a function of geographic longitude and latitude in the months of a year. TEC values presented were measured during HSA and 13:00–14:00 UT.

Table 2
Number of days with data.

Month	Solar activity level	Number of days
January	HSA	87
February	HSA	34
March	HSA	67
March	MSA	86
March	LSA	61
April	HSA	50
May	HSA	62
June	HSA	50
July	HSA	43
August	HSA	45
September	HSA	56
October	HSA	91
November	HSA	95
December	HSA	90

that during HSA there are increased ionizing radiations in X-ray and Extreme Ultra-Violet (EUV) bands, which in turn leads to increased TEC in the ionosphere (Hargreaves, 1992). In addition, during HSA, the temperature of the upper atmosphere increases by a factor of two (Hargreaves, 1992), leading to increased electron density at a given height. Figs. 3(a) and (b) demonstrate the existence of EIA region. The EIA features reported by previous studies (e.g Zhang et al. (2009), Bolaji et al. (2017), and Mungufeni et al. (2018)) are exhibited in the figures. For instance, the asymmetry of the EIA crests (Zhang et al., 2009) and the occurrence of several crests north and south of trough of EIA (Bolaji et al., 2017; Mungufeni et al., 2018). Moreover, Fig. 3 shows that locations outside the EIA region have the lowest TEC values compared to those within and around. This was also observed in Fig. 2 and then discussed.

3.3. Seasonal variation of TEC

Fig. 4 presents the variation of mean TEC values during 13:00–14:00 LT as a function of longitude and latitude. The month corresponding to the data is indicated on the respective panel. Due to space constraints, the months are abbreviated. The TEC values presented were those determined during HSA. As already stated in Section 3.2, the number of days with data in the months are presented in Table 2. The table shows that all the months have fairly adequate data (>30 days).

Several of the ionospheric features (spatial and EIA features) depicted in Fig. 4 have been discussed in Sections 3.1 and 3.2. Therefore, while discussing Fig. 4, we focused on the seasonal characteristics. It can be seen in Fig. 4 that the lowest TEC values occur in June and July (solstice months), while the highest occur in March, April and October (equinox months). At the moment, we may not explain the unexpectedly high values of TEC observed in the month of November. The results of the other months are

Please cite this article as: P. Mungufeni, B. A. Rabiu, D. Okoh et al., Characterisation of Total Electron Content over African region using Radio Occultation observations of COSMIC satellites, Advances in Space Research, https://doi.org/10.1016/j.asr.2019.08.009

similar to those reported by Akala et al. (2013), Olwendo et al. (2016) that were mentioned in Section 1. The ionosphere exhibits strong seasonal variations because the main source of ionization and energy for the ionosphere is photo-ionization which is seasonal dependent (Schunk and Nagy, 2009). The factors that control the source of ionisation (solar radiations) are the sub-solar point and the Sun-Earth distance. Zou et al. (2000) stated that an obvious possible cause of the annual anomaly is the 3% variation in Sun-Earth distance.

In June and December solstices, the sub-solar point is close to the region covered by geographic latitude ranges 20–26° and −26 to −20°, respectively. The closest and farthest distances between the Sun and Earth usually occur in January and July, respectively. Therefore, although the region covered by geographic latitude range 20–26° is close to the sub solar point in June solstice, the region does not receive maximum solar radiation. It follows that small TEC is measured over the region. Obviously, the region covered by geographic latitude range −26 to −20° which is far from the sub solar point in June solstice does not receive a lot of solar radiation. In general, over the region shown in Fig. 4, it is justified to observe small TEC in June solstice compared to other seasons.

The effect of the closeness of the region covered by geographic latitude range −26 to −20° to the sub-solar point can be seen in Fig. 4 in the months of December and January. Clearly, the TEC over geographic latitudes <−6° are mostly greater than those over latitudes >−6°. Much as the region covered by geographic latitude range 20–26° is far from the sub-solar point in December solstice, the region is influenced by the shortest distance between the Sun and the Earth in January. The reduced Sun-Earth distance results into an increased temperature which in turn results into increased O/N_2 ratio in the neutral air (Zou et al., 2000). Another result of increased atmospheric temperature is occurrence of interhemispheric transport of ionization (a global summer-to-winter thermospheric circulation). Sastri (1990), Gowtam and Tulasi R (2017) reported that at low latitudes, during solstices, the summer to winter hemispheric trans-equatorial neutral winds can transport the plasma from summer hemisphere to winter hemisphere causing higher plasma densities and intensified EIA crests in the winter hemisphere. This might explain the observation in Fig. 4 where over the region covered by geographic latitude range 20–26°, the TEC in December solstice exceeds that in June solstice.

By performing correlation analysis between coincident COSMIC and Ground TEC in Section 4 and quantifying the difference between the two data sets in Section 5, we validated COSMIC TEC.

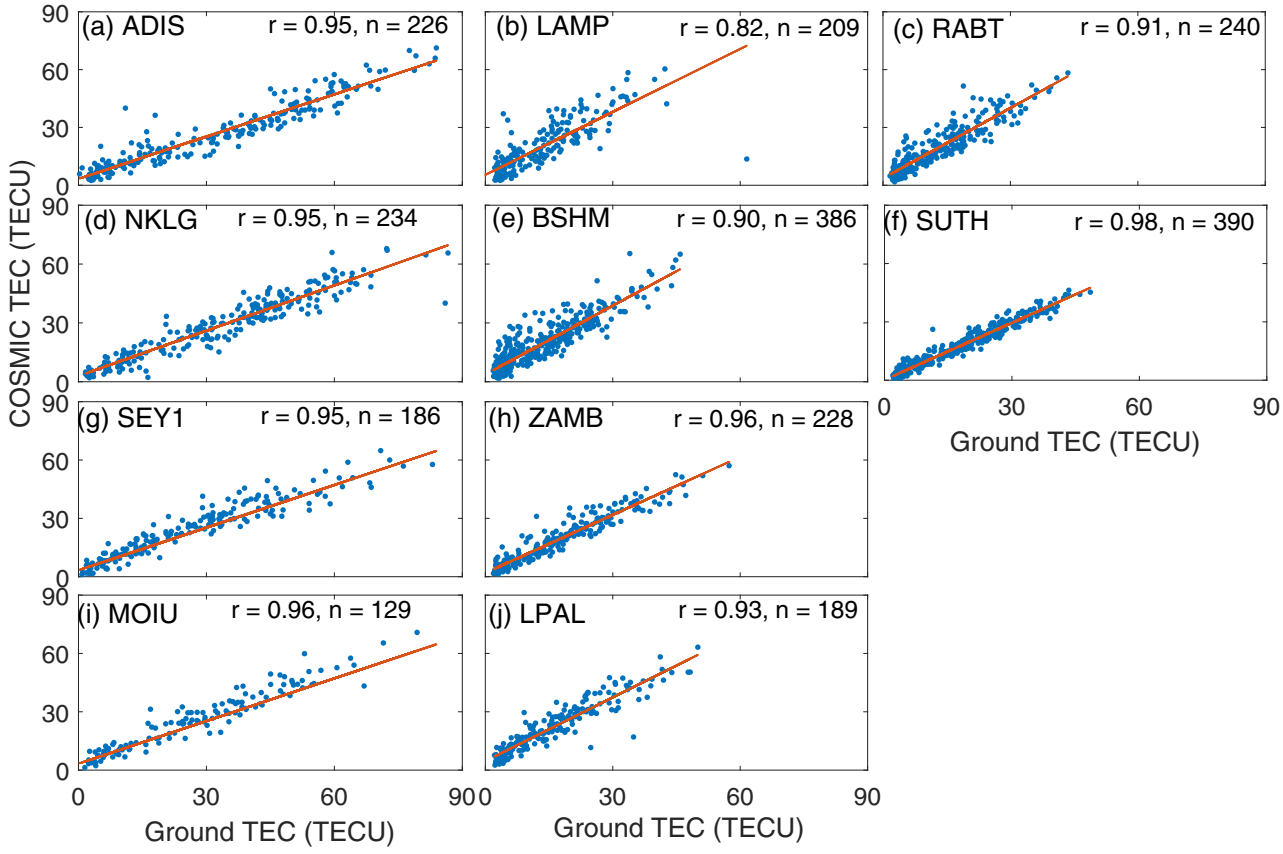


Fig. 5. Scatter plots of COSMIC TEC against Ground TEC over (a) ADIS, (b) LAMP, (c) RABT, (d) NKLG, (e) BSHM, (f) SUTH, (g) SEY1, (h) ZAMB, (i) MOIU, and (j) LPAL. r and n are the correlation coefficients and the number of pairs of data plotted, respectively.

Please cite this article as: P. Mungufeni, B. A. Rabiu, D. Okoh et al., Characterisation of Total Electron Content over African region using Radio Occultation observations of COSMIC satellites, Advances in Space Research, https://doi.org/10.1016/j.asr.2019.08.009

4. Correlation between COSMIC and Ground TEC

The COSMIC TEC values within geographic latitude and longitude ranges of 4 and 10 degrees, respectively centered over the IGS stations listed in Table 1 were separately binned at 1 h interval. TEC values within the bins were averaged to yield 1 h resolution TEC data over the stations. The Ground TEC over the IGS stations were similarly binned. It is important to note that the range of geographic latitude and longitude considered enabled us to use data of satellites with elevation angles $>25°$, thus minimising multi-path effects at low elevation angles.

Coincident COSMIC and Ground TEC were extracted and presented in Fig. 5. It is important to remind the reader that the data presented in Figs. 5 and 6 correspond to the years 2012 and 2015. On the panels for the various stations, the number of coincident TEC values, n are presented together with their correlation coefficients, r. Generally, the r values indicate reasonably good correlations ($r \geqslant 0.82$) between COSMIC and Ground TEC. This is an indication that both techniques of measuring TEC over a particular location track the same physical phenomena whose changes in turn results into the observed TEC. The equations of lines of best fits for the scatter plots in Fig. 5 are presented in Table 3.

In order to demonstrate that most points are close to the line of best fit in Fig. 5, we computed the root mean squared errors, RMSE, for each fit. The RMSE values are presented in Fig. 6. In the figure, the stations are arranged in the order of increasing magnetic latitude. It can be seen in Fig. 6, the RMSE values for stations at the southern mid latitude regions (SUTH and ZAMB) were well below 4 TECU, while for stations at the northern mid-latitude regions, most of the values were well above 5 TECU. Small values of RMSE indicate good fits and high values indicate the opposite. The general trend depicted in Fig. 6 is that the goodness of fit deteriorates from southern mid latitude to northern mid latitude region. The poor fits over low latitude stations could be due to the strong horizontal gradients in TEC over the EIA crests which are usually neglected during vertical profiling procedures (Garcia-Fernadez et al., 2002). However, the unexpected poor

Table 3
Equations of lines of best fits.

Station Code	Equation
ADIS	$y = 0.73x + 3.3$
LAMP	$y = 1.1x + 5.4$
NKLG	$y = 0.77x + 3$
RABT	$y = 1.2x + 3.6$
BSHM	$y = 1.2x + 3.7$
SEY1	$y = 0.74x + 4.8$
SUTH	$y = 0.98x + 0.24$
ZAMB	$y = 0.99x + 2$
MOIU	$y = 0.82x + 3.2$
LPAL	$y = 1.1x + 4.7$

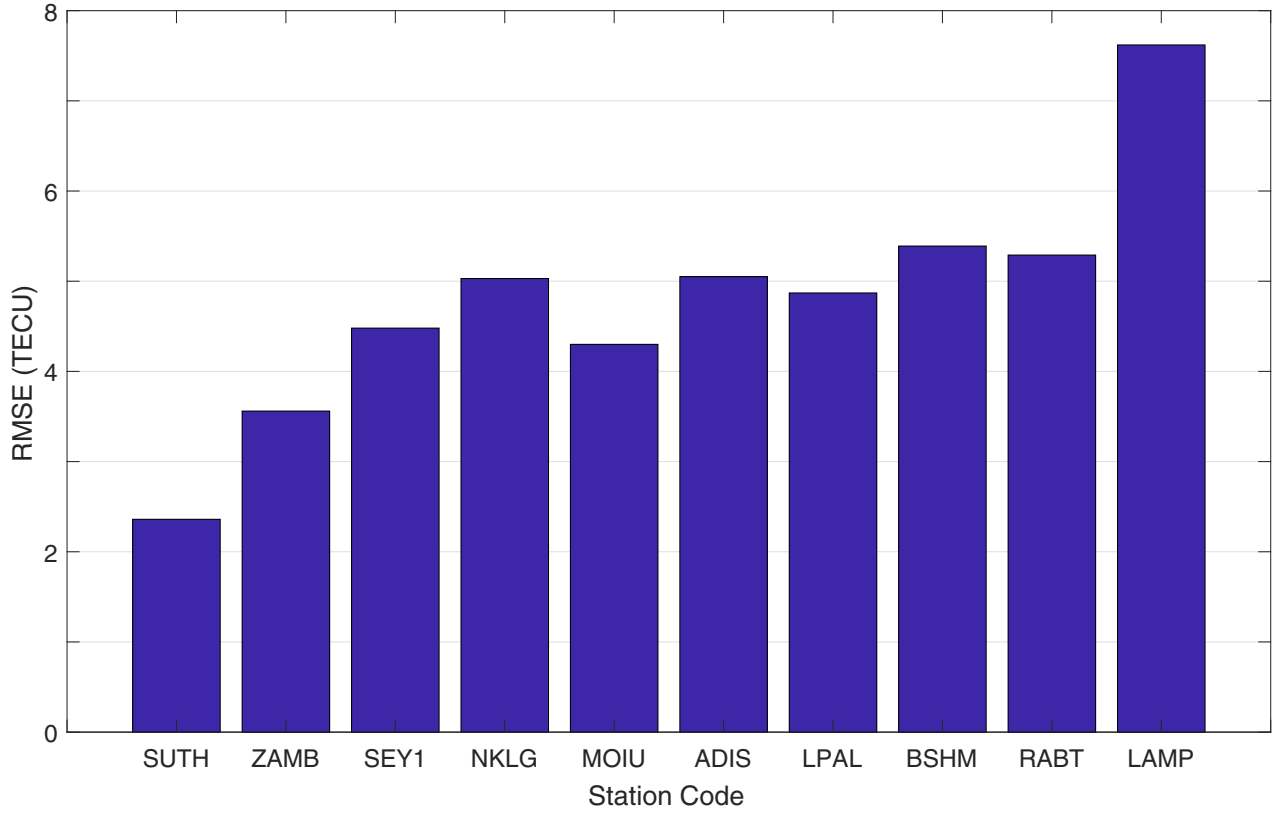


Fig. 6. Root Mean Squared errors over the IGS stations.

Please cite this article as: P. Mungufeni, B. A. Rabiu, D. Okoh et al., Characterisation of Total Electron Content over African region using Radio Occultation observations of COSMIC satellites, Advances in Space Research, https://doi.org/10.1016/j.asr.2019.08.009

goodness of fits observed over northern mid latitude stations needs further investigation.

Much as Fig. 5 has shown reasonably good correlation between COSMIC and Ground TEC, the RMSE values presented in Fig. 6 reveals that there are differences in coincident values in the two sets of data. In Section 5, these differences are quantified and used to reveal how COSMIC TEC compares with Ground TEC.

5. Differences between COSMIC and Ground TEC

The Ground TEC values that are plotted in Fig. 5 were subtracted from the corresponding COSMIC TEC. The differences were referred to as TEC differences. The TEC differences exist due to different path lengths of signals used to derive TEC. In the case of Ground TEC, the VTEC is derived from STEC which in turn is obtained from integrated electron density over 1 m^2 area. The integration is done from ground up to the location of GNSS satellite. For the case of COSMIC TEC, tangent points included in a particular occultation event have fairly large horizontal smear (up to thousands of kilometers). Therefore, electron density integration is done over a large area. Another reason for the TEC differences could be lack of inclusion of plasmaspheric TEC in COSMIC TEC. We computed as in Xiaohong and Long (2014) the plasmaspheric VTEC from the STEC available in podTec data files (http://cosmic-io.cosmic.ucar.edu/cdaac/index.html). The plasmaspheric VTEC were then binned into spatial and local time grids. The dimensions of the spatial grids and the resolution of local time grids were similar to that of COSMIC TEC mentioned in Section 3. The coincident plasmaspheric VTEC and COSMIC TEC were added. Although we have not presented the results here, the addition of plasmaspheric VTEC onto COSMIC TEC amplified the TEC differences which were already positive, while the negative values were increased close to zero. Due to the amplification of the TEC differences and the reduction of correlation coefficients between COSMIC and Ground TEC, we did not add plasmaspheric TEC to COSMIC TEC.

Fig. 7 presents the variation of the number of observed TEC differences. In the figure, panels (a)–(f) present the number of observed TEC differences over ADIS, LAMP, NKLG, RABT,SEY1, and SUTH, respectively. To avoid clumsiness on the horizontal axis, the ranges of the bars are not indicated. However, it can be noted that, the bars have ranges of 4 TECU. For example, a bar at −4 has a range of −6 to −2 TECU. On the right upper corner of the panels in Fig. 7, the upper quartiles, UQ, of the magnitudes of the TEC differences observed over the respective stations are indicated. The UQ values enabled us to determine the dominant high values of TEC differences over the respective stations. The program that computes UQ of data vector x which has n elements by first sorting the data in

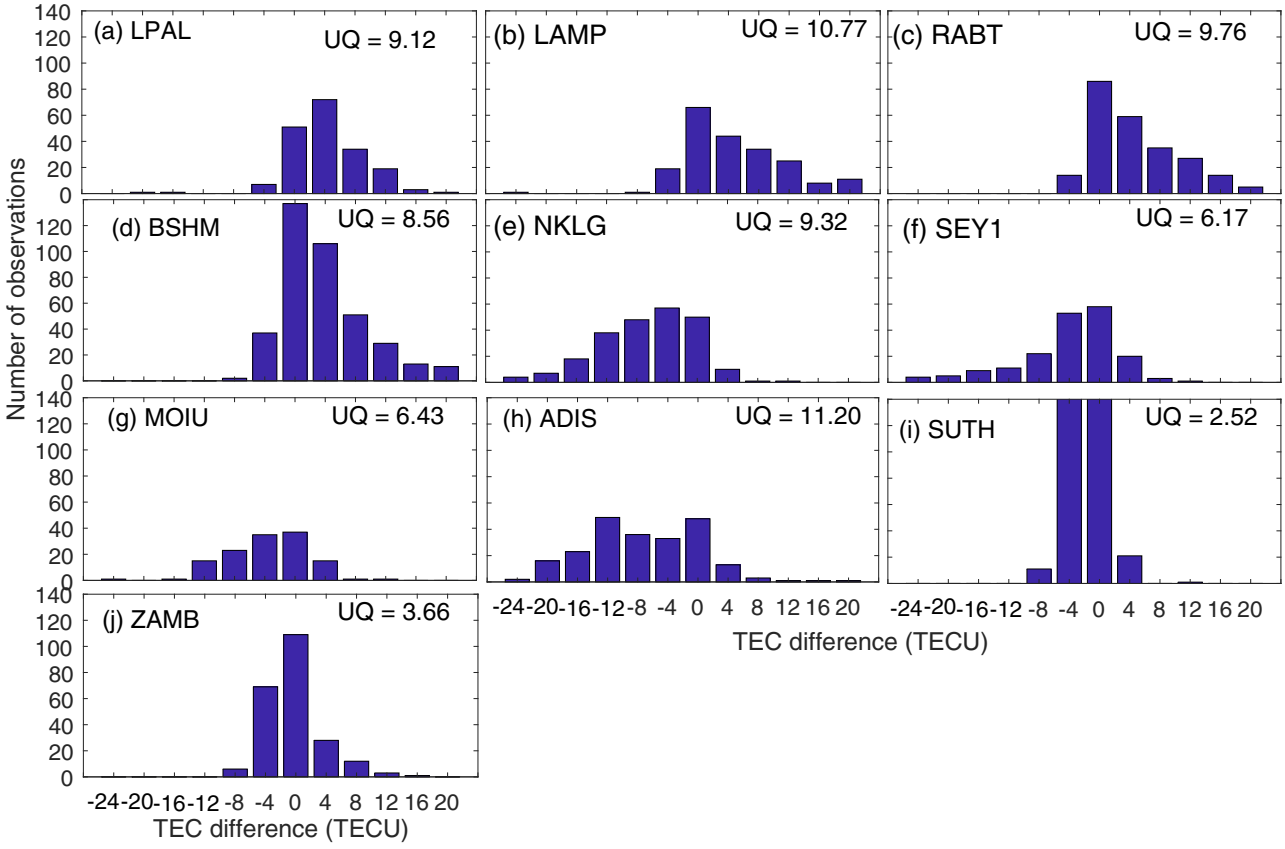


Fig. 7. Variation of the number of observed TEC differences over (a) LPAL, (b) LAMP, (c) RABT, (d) BSHM, (e) NKLG, (f) SEY1, (g) MOIU, (h) ADIS, (i) SUTH, and (j) ZAMB.

Please cite this article as: P. Mungufeni, B. A. Rabiu, D. Okoh et al., Characterisation of Total Electron Content over African region using Radio Occultation observations of COSMIC satellites, Advances in Space Research, https://doi.org/10.1016/j.asr.2019.08.009

ascending order. It then assigns quantiles to the sorted numbers as, $0.5/n, 1.5/n, \ldots, (n-0.5)/n$. The value of sorted x that corresponds to 3/4 quantile, $y_{(3/4)}$ is obtained by linear interpolation as;

$$y_{(3/4)} = y_b + \frac{3/4 - b}{a - b} \times (y_a - y_{(3/4)}), \quad (1)$$

where a and b are quantile values after and before 3/4, respectively, while y_a and y_b are the corresponding sorted values of x.

It can be seen from Fig. 7 that, most of the TEC differences over southern mid latitude stations are distributed over a small range (from −6 to 6 TECU) that is approximately centered at 0 TECU. This observation is consistent with the low UQ values (< 4 TECU) observed over these stations. Moreover, Fig. 6 also showed good fits over southern mid-latitude regions. Fig. 7 shows that, the UQ values over low latitude (ADIS, NKLG, MOIU, and SEY1) and northern mid-latitude (LPAL, RABT, LAMP, BSHM) regions range from 6.17 to 11.20 TECU. This result is similar to that reported by Tsai et al. (2001) when they compared electron density profiles derived using MicroLab 1 RO with those observed by ionograms of digital ionospheric sounders. They found that the comparisons between F2-layer critical frequency (foF2) from the two sources were better at mid-latitudes than at low-latitudes. Tsai et al. (2001) stated that, the high TEC differences over low latitude regions compared to those over southern mid latitudes could have resulted from errors due to the spherical symmetry assumption during the RO retrievals.

Another observation that can be made from Fig. 7 is that the TEC differences over the northern mid-latitude regions are mostly positive, while those over the low latitude regions are mostly negative. Based on the definition of TEC difference given earlier, positive values signify that COSMIC TEC is greater than Ground TEC. More time and data is needed in order to explain the observation of TEC differences over the northern mid-latitude regions being strongly positive, while those over the low-latitude regions being negative. However, the TEC differences over low-latitude regions which were strongly negative could be due to errors in electron density retrieval.

6. Conclusions

We characterised TEC over the African region using COSMIC TEC. The well known features of TEC reproduced by COSMIC TEC included: (i) occurrence of minimum and maximum TEC during 0:00–08:00 LT and 12:00–16:00 LT respectively, (ii) occurrence of a secondary maximum/enhancement during 16:00–20:00 LT, (iii) lowest TEC values being observed in June solstice and highest TEC values observed in March equinox and December solstice, (iv) TEC values increase as solar activity changes from low to high, (v) mid latitude TEC values are lower than those of low latitude regions, and (vi) there is occurrence of equatorial ionisation anomaly.

The correlations between simultaneously observed COSMIC and Ground TEC, over 10 IGS stations distributed over the African region were done. The correlation coefficients indicated fairly high correlations ($\geqslant 0.82$) between COSMIC and Ground TEC. The goodness of fits over low and northern mid-latitude regions were poor compared to those over southern mid latitude. This was attributed to the strong horizontal gradients in TEC over the EIA crests which are usually neglected during vertical profiling procedures. TEC differences between coincident Ground and COSMIC TEC were observed to be highest over low and northern mid-latitude regions compared to those over mid-latitudes. The findings of this study are important as they have justified future use of COSMIC TEC for empirical modeling over Africa.

Acknowledgments

The International Science program of Sweden financially, supported this study.

The data used in this study were obtained from, http://www.sopac.ucsd.edu and http://cosmic-io.cosmic.ucar.edu/cdaac/index.html.

References

Adewale, A.O., Oyeyemi, E.O., Adeloye, A.B., Ngwira, C.M., Athieno, R., 2011. Responses of equatorial F region to different geomagnetic storms observed by GPS in the African sector. J. Geophys. Res. 116, A12319. https://doi.org/10.1029/2011JA016998.

Adewale, A.O., Oyeyemi, E.O., Cilliers, P.J., McKinnell, L.A., Adeloye, A.B., 2012. Low solar activity variability and IRI 2007 predictability of equatorial Africa GPS TEC. Adv. Space Res. 49, 316–326.

Akala, A.O., Seemala, G.K., Doherty, P.H., Valladares, C.E., Carrano, C. S., Espinoza, J., Oluyo, S., 2013. Comparison of equatorial GPS-TEC observations over an African station and an American station during the minimum and ascending phases of solar cycle 24. Ann. Geophys. 31, 2085–2096.

Batista, I.S., Abdu, M.A., Bittencourt, J.A., 1986. Equatorial F region vertical plasma drifts: seasonal and longitudinal asymmetries in the American sector. J. Geophys. Res. 91 (A11), 12055–12064.

Bolaji, O., Owolabi, O., Falayi, E., Jimoh, E., Kotoye, A., Odeyemi, O., Rabiu, B., Doherty, P., Yizengaw, E., Yamazaki, Y., Adeniyi, J., Kaka, R., Onanuga, K., 2017. Observations of equatorial ionization anomaly over Africa and Middle East during a year of deep solar minimum. Ann. Geophys. 35, 123–132.

Buonsanto, M.J., 1999. Ionospheric storms – a review. Space Sci. Rev. 88, 563–601.

Chen-Joe, F., 2008. Constellation deployment for the FORMOSAT-3/COSMIC mission. IEEE Trans. Geosci. Remote Sens. 46 (11), 3367–3379.

Garcia-Fernadez, M., Hernandez-Pajares, M., Juan-Zornoza, J.M., Sanz-Subirana, J., 2002. An improvement of retrieval techniques for ionospheric radio occultations. In: Reigber, C., Ltihr, H., Schwintzer, P. (Eds.), First CHAMP Mission Results for Gravity, Magnetic and Atmospheric Studies. Springer-Verlag, pp. 430–440.

Gowtam, S.V., Tulasi R, S., 2017. Ionospheric winter anomaly and annual anomaly observed from Formosat-3/COSMIC Radio Occultation observations during the ascending phase of solar cycle 24. Adv. Space Res. https://doi.org/10.1016/j.asr.

Please cite this article as: P. Mungufeni, B. A. Rabiu, D. Okoh et al., Characterisation of Total Electron Content over African region using Radio Occultation observations of COSMIC satellites, Advances in Space Research, https://doi.org/10.1016/j.asr.2019.08.009

Hargreaves, J.K., 1992. The Solar-Terrestrial Environment. Cambridge University Press, The Pitt building, Trumpington Street, Cambridge CB2 IRP.

Hoque, M.M., Jakowski, N., 2012. A new global model for the ionospheric F2 peak height for radio wave propagation. Ann. Geophys 30, 797–809.

Jakowski, N., Leitinger, R., Angling, M., 2004. Radio occultation techniques for probing the ionosphere. Ann. Geophys. 47 (2/3), 1049–1066.

Krankowski, A., Zakharenkova, I., Krypiak-Gregorczyk, A., Shagimuratov, I., Wielgosz, P., 2011. Ionospheric electron density observed by FORMOSAT-3/COSMIC over the European region and validated by ionosonde data. J. Geod 85, 949–964.

Kuo, Y.H., Wee, T.K., Sokolovskiy, S., Rocken, C., Schreiner, W., Hunt, D., Anthes, R.A., 2003. Inversion and error estimation of GPS radio occultation data. J. Meteorol. Soc. Jpn. 82 (1B), 507–531.

Mungufeni, P., Habarulema, J.B., Migoya-Orué, Y., Jurua, E., 2018. Statistical analysis of the correlation between the equatorial electrojet and the occurrence of the equatorial ionisation anomaly over the East African sector. Ann. Geophys. 36, 841–853.

Mungufeni, P., Jurua, E., Habarulema, J.B., Anguma, S.K., 2015. Modeling the probability of ionospheric irregularity occurrence over African low latitude region. J. Atmos. Sol.-Terr. Phys. 128, 46–57.

Obrou, O.K., Mene, M.N., Kobea, A.T., Zaka, K.Z., 2009. Equatorial total electron content (TEC) at low and high solar activity. Adv. Space Res. 43, 1757–1761.

Olwendo, O.J., Yamazaki, Y., Cilliers, P.J., Baki, P., Doherty, P., 2016. A study on the variability of ionospheric total electron content over the East African low-latitude region and storm time ionospheric variations. Radio Sci. 51, 1757–1761.

Pedatella, N.M., Yue, X., Schreiner, W.S., 2015. An improved inversion for FORMOSAT-3/COSMIC ionosphere electron density profiles. J. Geophys. Res. Space Phys 120, 8942–8953. https://doi.org/10.1002/2015JA021704.

Risbeth, H., Garriot, O.K., 1969. Introduction to Ionospheric Physics. Academic Press, Inc., III Fifth Avenue, New York, New York 10003.

Sastri, J.H., 1990. Equatorial anomaly in F-region – A review. Indian J. Radio Space Phys. 19, 225–240.

Schunk, W.R., Nagy, F.A., 2009. Ionospheres: Physics, Plasma Physics, and Chemistry, 2nd ed. Cambridge University Press, New York, USA.

Seemala, G., Valladares, C., 2011. Statistics of total electron content depletions observed over the South American continent for the year 2008. Radio Sci. 46. https://doi.org/10.1029/2011RS004722.

Syndergaard, S., Schreiner, W.S., Rocken, C., Hunt, D.C., Dymond, K. F., 2006. Preparing for cosmic: Inversion and analysis of ionospheric data products. In: Foelsche, U., Kirchengast, G., Steiner, A.K. (Eds.), Atmosphere and Climate: Studies by Occultation Methods. Springer, New York, pp. 137–146.

Tsai, L.-C., Tsai, W.H., Schreiner, W.S., Berkey, F.T., Liu, J.Y., 2001. Comparisons of GPS/MET retrieved ionospheric electron density and ground based ionosonde data. Earth Planets Space 53, 193–205.

Xiaohong, Z., Long, T., 2014. Daily Global Plasmaspheric Maps Derived From COSMIC GPS Observations. IEEE Trans. Geosci. Remote Sens. 52 (10), 6040–6046.

Yue, X., Schreiner, W., Kuo, Y., Lei, J., 2015. Ionosphere equatorial ionization anomaly observed by GPS radio occultations during 2006–2014. J. Atm. Sol-Terr. Phys. 129, 30–40.

Zhang, M.-L., Wan, W., Liu, L., Ning, B., 2009. Variability study of the crest-to-trough TEC ratio of the equatorial ionization anomaly around 120°E longitude. Adv. Space Res. 43, 1762–1769.

Zou, L., Rishbeth, H., Müller-Wodarg, I.C.F., Aylward, A.D., Millward, G.H., Fuller-Rowell, T.J., Idenden, D.W., Moffett, R.J., 2000. Annual and semiannual variations in the ionospheric F2-layer. I. Modelling. Ann. Geophysicae 18, 927–944.

Please cite this article as: P. Mungufeni, B. A. Rabiu, D. Okoh et al., Characterisation of Total Electron Content over African region using Radio Occultation observations of COSMIC satellites, Advances in Space Research, https://doi.org/10.1016/j.asr.2019.08.009